Chemical Research in Toxicology

ARTICLE

pubs.acs.org/crt

Pulmonary Toxicity and Metabolic Activation of Tetrandrine in CD-1 Mice

Hua Jin,[†,§] Liang Li,[‡,§] Dafang Zhong,[‡] Jia Liu,[‡] Xiaoyan Chen,[*,‡] and Jiang Zheng[*,†]

[†]Center for Developmental Therapeutics, Seattle Children's Research Institute, Division of Gastroenterology and Hepatology, Department of Pediatrics, University of Washington, Seattle, Washington 98101, United States

[‡]Shanghai Institute of Materia Medica, Chinese Academy of Sciences, Shanghai, China

Supporting Information

ABSTRACT:

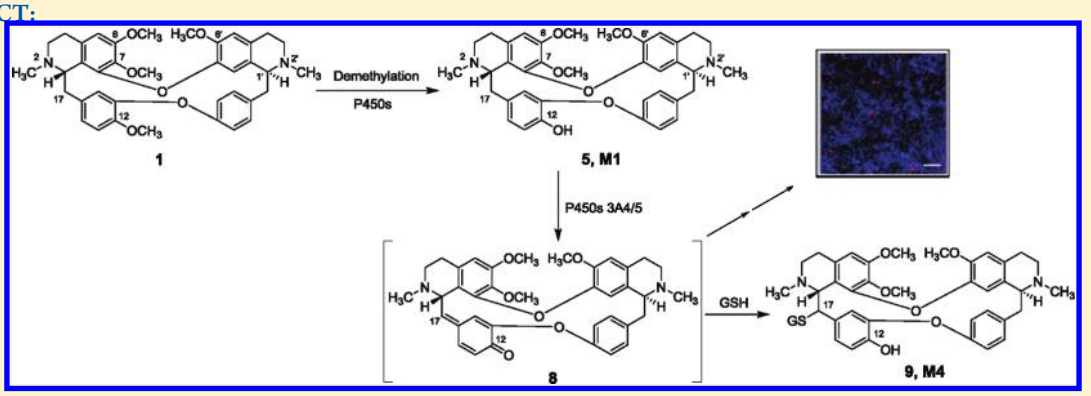

Tetrandrine, a bisbenzylisoquinoline alkaloid, has demonstrated promising pharmacologic activities. The alkaloid has a great potential for clinical use, so a careful, thorough toxicity evaluation of the alkaloid is required. In the present study, 24 h acute toxicity of tetrandrine was evaluated in CD-1 mice. Single intraperitoneal doses of tetrandrine at 150 mg (0.24 mmol)/kg were found to cause alveolar hemorrhage and over 3-fold elevation of lactate dehydrogenase activity in bronchoalveolar lavage fluids. Ethidium-based staining showed loss of membrane integrity in significant numbers of cells in the lungs of the animals treated with the same doses of tetrandrine. As much as 60% reduction in cell viability was observed after 24 h of exposure to tetrandrine at 40 μM in human lung cell lines NL-20 and WI-38. Ketoconazole, an inhibitor of P450 3A, showed a protective effect on the pulmonary injury in mice given tetrandrine. A glutathione (GSH) conjugate derived from *O*-demethylated tetrandrine was detected in incubations of tetrandrine with NADPH- and GSH-supplemented human liver and mouse lung microsomes. The electrophilic metabolite trapped by GSH is considered to be a quinone methide derivative. The formation of the metabolite reactive to GSH was found to require the presence of NADPH. The coincubation of ketoconazole suppressed the generation of the GSH conjugate. Tetrandrine was incubated with a selection of recombinant human cytochrome P450 enzymes, and only P450s 3A4 and 3A5 were responsible for the production of the reactive metabolite. The results implicate a possible correlation between the formation of the quinone methide metabolite of tetrandrine and the pulmonary toxicity induced by tetrandrine.

INTRODUCTION

Bisbenzylisoquinoline alkaloids have been the subject of extensive investigations, particularly in the last two decades, because of their promising and diverse biological activities—anti-inflammatory, antitumor, antitubercular, and antiplasmodial effects.[1−9] More than 400 of these alkaloids have been identified in plants of 12 families.[9] These are usually formed by two benzylisoquinoline units linked by one or more ether bridges or, rarely, carbon−carbon bridges. The substituents on the *para* position of aromatic rings in these structures are usually hydroxyl or methoxyl or (less often) methylenedioxyl groups.

Tetrandrine (**1**, Scheme 1) is a representative of diaryl ether type bisbenzylisoquinoline alkaloids and is the major bioactive component isolated from the root of *Stephenia tetrandra* S Moore.[10] A number of studies have demonstrated that tetrandrine possessed multiple bioactivities, including anti-inflammation,[11] immunomodulation,[12,13] reversion of cardiac and vascular remodeling,[10,14] inhibition of hepatic fibrosis[15−17] and hepatoprotection,[18] suppression of tumor proliferation,[19−21] and multidrug resistance.[22−27] The alkaloid has also been used in the treatment of ischemic heart diseases, hypertension, and silicosis in China. The pharmacologic activities of tetrandrine are evident in animals, but whether this alkaloid is safe for clinical use has not been evaluated sufficiently. Li et al. demonstrated that continuous administration of tetrandrine induced liver injury in dogs.[28] Cai et al.

Received: July 16, 2011
Published: October 12, 2011

ACS Publications © 2011 American Chemical Society

Scheme 1. Chemical Structures of Tetrandrine (1), Fangchinoline (2), Berbamine (3), Dauricine (4a), and Quinone Methide of Dauricine (4b)

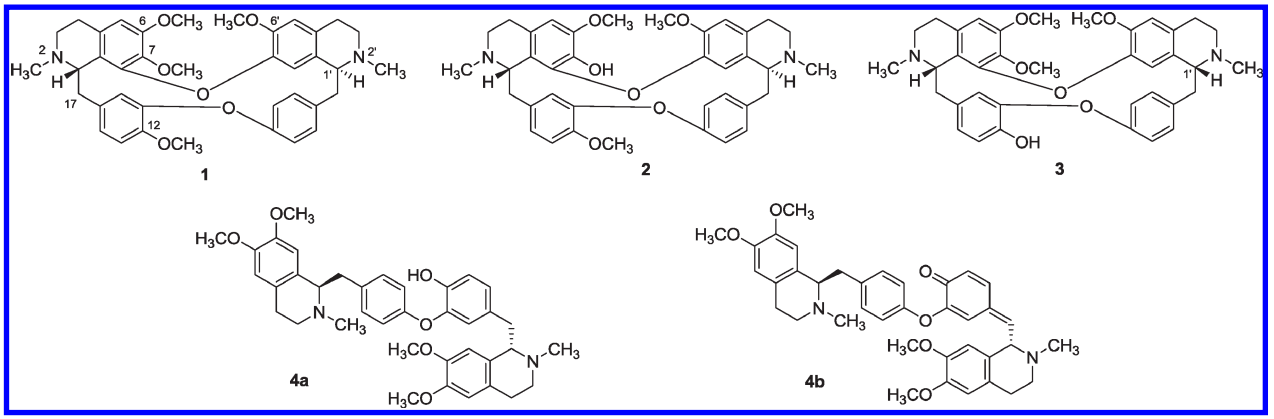

reported apoptosis and mitochondrial dysfunction induced by tetrandrine in liver of Sprague−Dawley rats.[29]

The objectives of the present study included (1) evaluation of acute liver injury and pulmonary toxicity of tetrandrine, (2) characterization of reactive metabolites of tetrandrine, (3) identification of cytochrome P450 (P450) enzymes responsible for the bioactivation of tetrandrine, and (4) investigation of the correlation between the formation of reactive metabolites of tetrandrine and pulmonary toxicity induced by tetrandrine.

MATERIALS AND METHODS

Chemicals and Materials. Tetrandrine, fangchinoline (**2**, Scheme 1), and berbamine (**3**) were purchased from Shenzhen Medherb Bio-Tech Co., Ltd. (Shenzhen, Guangdong, China). All purities were >98%. Ethidium homodimer-III (EthD-III) was purchased from Biotium (Hayward, CA), and 4′-6-diamidino-2-phenylindole (DAPI) was purchased from Vector Laboratories (Burlingame, CA). Glutathione, α-naphthoflavone, sulfaphenazole, ticlopidine, quinidine, chlormethiazole, ketoconazole, and formaldehyde solution were purchased from Sigma-Aldrich (St. Louis, MO). Gentamicin, media Dulbecco's modified Eagle's medium (DMEM)/F12 and RPMI-1640, and trypsin were purchased from Mediatech (Herndon, VA). Hematoxylin and eosin were purchased from Fisher Scientific (Fair Lawn, NJ). Low melting point agarose and D-luciferin were purchased from Promega (Madison, WI). Recombinant human P450 enzymes were purchased from BD Gentest (Woburn, MA). 4-Ipomeanol was kindly provided from National Cancer Institute (Frederick, MD). All other reagents and solvents were of either analytical or HPLC grade.

Animals and Treatment. Male CD-1 mice (20−22 g) were obtained from Charles River Laboratories (Wilmington, MA). All mice were kept in accordance with National Institutes of Health (NIH) guidelines for animal care and the guidelines of Seattle Children's Research Institute and maintained at a specific pathogen-free facility. Stock solutions of tetrandrine were prepared as follows. Tetrandrine (18.0 mg) was suspended in 0.5 mL of water, and the resulting suspension was acidified by adding dilute HCl solution until tetrandrine was dissolved. The resultant solution was neutralized with dilute NaOH solution, followed by the addition of water to the appropriate concentrations. For the toxicity test of tetrandrine, the animals were divided into four groups, and each group contained six mice. One group was treated intraperitoneally (ip) with saline as the vehicle control, and the other groups were treated with tetrandrine at dosages of 50, 100, and 150 mg/kg, respectively. The animals were sacrificed 24 h after the administration. Following anesthesia with pentobarbital, blood was harvested by cardiac puncture for alanine aminotransferase (ALT) and aspartate aminotransferase (AST) assays. In a separate study, mice were treated ip with ketoconazole (50 mg/kg). After 1.5 h of the administration, the animals were given ip tetrandrine at 150 mg/kg and sacrificed 24 h after the treatment.

Bronchoalveolar Lavage (BAL) Fluid Collection. Lavage fluid collection was conducted following the protocol previously published by our laboratory.[30] Briefly, mice were anesthetized, and the trachea was exposed and cannulated with a feeding needle tied in place. The lungs were perfused with phosphate-buffered saline (PBS) via right ventricle into the pulmonary artery to remove blood from the lungs. The lungs were lavaged with PBS buffer, and the recovered fluids were centrifuged at 1500*g* for 15 min at 4 °C. The supernatants were subjected to the assessment of lactate dehydrogenase (LDH) activity.

ALT and AST Assays. The blood samples collected above were allowed to clot in test tubes at room temperature overnight, followed by centrifugation at 1000*g*. The resulting sera were collected for ALT and AST assays. Serum ALT and AST activities were measured by following the manufacturer's instruction (Catachem Inc., Bridgeport, CT).

LDH Activity and Protein Assays. The activity of LDH in BAL fluids harvested was measured by In Vitro Toxicology Assay kit from Sigma-Aldrich. The specific activity was based on protein concentrations as determined using bicinchoninic acid protein assay kit (Pierce Inc., Rockford, IL).

Histopathological Analysis. The lung tissues were fixed in 10% neutral buffered formalin, paraffin processed, and sectioned at 3 μm. For histological analysis, the tissue sections were stained with hematoxylin and eosin (H&E).

Cell Permeability. Lung cell membrane integrity was evaluated, according to the method described in our previous publication.[30] Briefly, mice were anesthetized with pentobarbital. The trachea was exposed and cannulated with a feeding needle tied in place. The lungs were lavaged two times with a solution of fluorescent dyes EthD-III (2.0 μM) and then DAPI (300 μM) and inflated with the same solution for 20 min. The unbound dyes were then removed by lavaging with PBS buffer twice. The lungs were harvested, embedded in Tissue-Tek OCT (Sakura Finekek USA Inc., Torrance, CA), and quickly frozen in liquid nitrogen. The frozen lung tissues were cut into 5 μm thick slices and placed on glass slides. After they were fixed in cold acetone (−20 °C) for 2 min, the cryostat slices were mounted with water-based mounting media under glass coverslips. Representative areas were photographed with a Zeiss Axiovert 200 M fluorescence microscope.

Microdissection of Airway Segment and Culture. Microdissection of airway segments and tissue cultures were performed as

described by our laboratory.[30] Briefly, animals were anesthetized with pentobarbital. The lungs were inflated with 1% low-melting agarose gel, harvested, and immersed in DMEM/F12 medium during dissection. The distal airway branches were dissected starting from their branch-point with the major daughter airway to the most distal terminal bronchioles. The resulting dissected lung airways were gently washed with PBS buffer to remove agarose possibly remaining within the tissues and then incubated with 4-ipomeanol or tetrandrine in serum-free DMEM/F12 medium supplemented with gentamicin (50 μg/mL). After 24 h of incubation, the media were saved for LDH assay, the airways were homogenized, and the lysates were collected for protein assay.

Cell Culture and Cell Viability Assay. Human pulmonary cell lines WI-38 and NL-20 were incubated in medium DMEM/F12, respectively, supplemented with 10% FBS and gentamicin (50 μg/mL). Cells were seeded in 96-well plates at a density of 1×10^4/well and exposed to tetrandrine at designated concentrations. The resulting cells were cultured at 37 °C in a humidified incubator with 95% air/5% CO_2. The cell viability was determined using CellTiter 96 Aqueous One cell proliferation assay (Promega) based on the protocol provided by the manufacturer.

Microsomal Incubations. Human liver microsomes (HLMs) were purchased from BD Gentest, and CD-1 mouse lung microsomes were prepared as described by our laboratory.[30,31] Microsomal incubations were conducted at 37 °C for 60 min. A stock solution of tetrandrine was prepared in methanol. The final reaction mixtures contained 1 mg/mL human liver microsomal protein (or mouse lung microsomal protein), 3 mM NADPH, 50 μM tetrandrine, and 2.5 mM glutathione (GSH). Control samples with no NADPH, no trapping agent (i.e., GSH), or no test compound were performed. Incubation reaction mixtures were brought to a final volume of 200 μL with 100 mM potassium phosphate buffer (pH 7.4). An equal volume of ice-cold acetonitrile was used to terminate the incubation reactions. To a 200 μL aliquot of incubation samples, 400 μL of methanol was added. This mixture was vortex-mixed and centrifuged to remove precipitated protein at 14000*g* for 5 min. The supernatant was evaporated to dryness under a stream of nitrogen at 40 °C and then reconstituted in 100 μL of methanol:5 mM ammonium acetate:formic acid (30:70:0.1, v/v/v). A 20 μL aliquot of the reconstituted solution was injected to liquid chromatography/ion trap mass spectrometry (LC/MS^n) for analysis. Each incubation was performed in duplicate.

In a separate study, an up-scaled human liver microsomal incubation with tetrandrine was performed (5 mL) under similar experimental conditions as described above. After 60 min of incubation, the reaction was quenched with equal volume of ice-cold acetonitrile, followed by centrifugation at 14000*g* for 5 min. The resulting supernatants were concentrated by evaporation under a stream of nitrogen and subjected to HPLC separation. The fractions with retention times at 11.2 (M1) and 12.4 min (M2) were collected and pooled, respectively. The pooled fractions containing either M1 or M2 were divided into three equal parts accordingly, then evaporated to dryness under a stream of nitrogen at 40 °C, and individually incubated with mouse lung microsomes (1 mg/mL) in the presence or absence of NADPH (3 mM) or in the presence of NADPH and ketoconazole (1.0 μM), respectively. All microsomal reactions contained GSH (2.5 mM) as a trapping agent.

Recombinant Human P450 Incubations. Conditions were equivalent to the microsomal incubations except that microsomes were replaced by individual human recombinant P450 enzymes (50 nM), including P450s 1A2, 1B1, 2A6, 2B6, 2C8, 2C9, 2C19, 2D6, 2E1, 3A4, 3A5, and 4A11.

Metabolizing Enzyme Inhibition Studies. To determine the specific cytochrome P450 enzymes involved in the formation of reactive metabolites, a total of six P450 inhibitors were tested as follows: α-naphthoflavone (0.1 μM for P450 1A2), sulfaphenazole (1.0 μM for P450 2C9), ticlopidine (0.4 μM for P450 2B6 and 6.0 μM for P450 2C19), quinidine (2.0 μM for P450 2D6), chlormethiazole (60 μM for P450 2E1), and ketoconazole (1.0 μM for P450 3A4/5). The production of GSH conjugates was monitored and quantitated by LC/MS^n method as below. Incubation mixtures contained 1 mg/mL pooled HLMs, 50 μM tetrandrine, 3 mM NADPH, 2.5 mM GSH, and the inhibitors at various concentrations in 100 mM potassium phosphate buffer (pH 7.4). The final incubation volume was 0.2 mL. Incubations were performed at 37 °C for 30 min, and reactions were terminated by an equal volume of ice-cold acetonitrile. Controls containing no chemical inhibitors were included. In a separate incubation, ketoconazole (1.0 μM) was incorporated into mouse lung microsomes before the addition of NADPH and GSH. Each incubation was performed in duplicate.

LC/MS^n Method. Metabolites were separated and characterized on an Agilent 1200 HPLC system coupled with a 6330 LC/MSD Trap XCT Ultra mass spectrometer (Agilent Technologies, Waldbronn, Germany). Separation was achieved using a Zorbax XDB-C_8 column (150 mm × 4.6 mm i.d., 5 μm; Agilent, Wilmington, DE) protected by a 4.0 mm × 3.0 mm i.d. Security-Guard (5 μm) C_{18} column (Phenomenex, Torrance, CA). The following gradient was used at a flow rate of 0.5 mL/min: initial 30% A maintained for 3 min, then increased to 42% in 17 min, then increased to 100% in 0.1 min, maintained at 100% for 5 min, and finally decreased to 30% A in 0.1 min, maintained at 30% A for 8 min. Solvent A was methanol containing 0.1% formic acid; solvent B was 5 mM ammonium acetate containing 0.1% formic acid. Full scan MS analysis was performed with electrospray ionization (ESI) in the positive mode. The MS/MS and MS^3 spectra were produced by collision-induced dissociation (CID) of the single-charged ion $[M + H]^+$ or double-charged ion $[M + 2H]^{2+}$ of all analytes. The interface voltage was 3.5 kV, the nebulizer gas (N_2) pressure was 50 psi, the dry gas flow was 12 L/min, and the heated block temperature was 350 °C. All data acquired were processed by Agilent ChemStation Rev. B. 01.03 software (Agilent, Palo Alto, CA).

Data Analysis. All results are given as means ± SEs. The results were analyzed by Student's *t* test (GraphPad software, San Diego, CA). A value of $p < 0.05$ was considered significant (*), and $p < 0.01$ was highly significant (**) as compared to the corresponding control.

RESULTS

LDH Activity in BAL Fluids. To evaluate the pulmonary toxicity, the LDH activity in BAL fluids was determined 24 h following ip administration of tetrandrine. As shown in Figure 1A, treatment of tetrandrine in mice at 150 mg/kg (0.24 mmol/kg) produced over 3-fold elevation of LDH activity in BAL fluids.

Histology and Pulmonary Cell Membrane Permeability. Histopathologic changes of lungs of mice were monitored. Massive bronchiolar and alveolar hemorrhage and edema were observed in the animals given tetrandrine at dose of 150 mg/kg (Figure 1B). Both alveolar ducts and terminal bronchioles were filled with hemorrhage and eosinophilic exudate. To image the pulmonary injury induced by tetrandrine, the lungs were stained with EthD-III and DAPI. Increased numbers of ethidium-positive (shown in red in Figure 1C) cells were observed in the lungs obtained from the animals treated with tetrandrine at the dose of 150 mg/kg. The loss of membrane integrity showed dose dependency for tetrandrine exposure (Figure 1C).

Distal Airway Incubation and Tissue Injury. To examine direct toxic effects of tetrandrine on distal airway tissues, mouse lungs were dissected, and distal airways were harvested and incubated with tetrandrine, followed by monitoring LDH released to the media. About 2-fold increase in LDH activity was

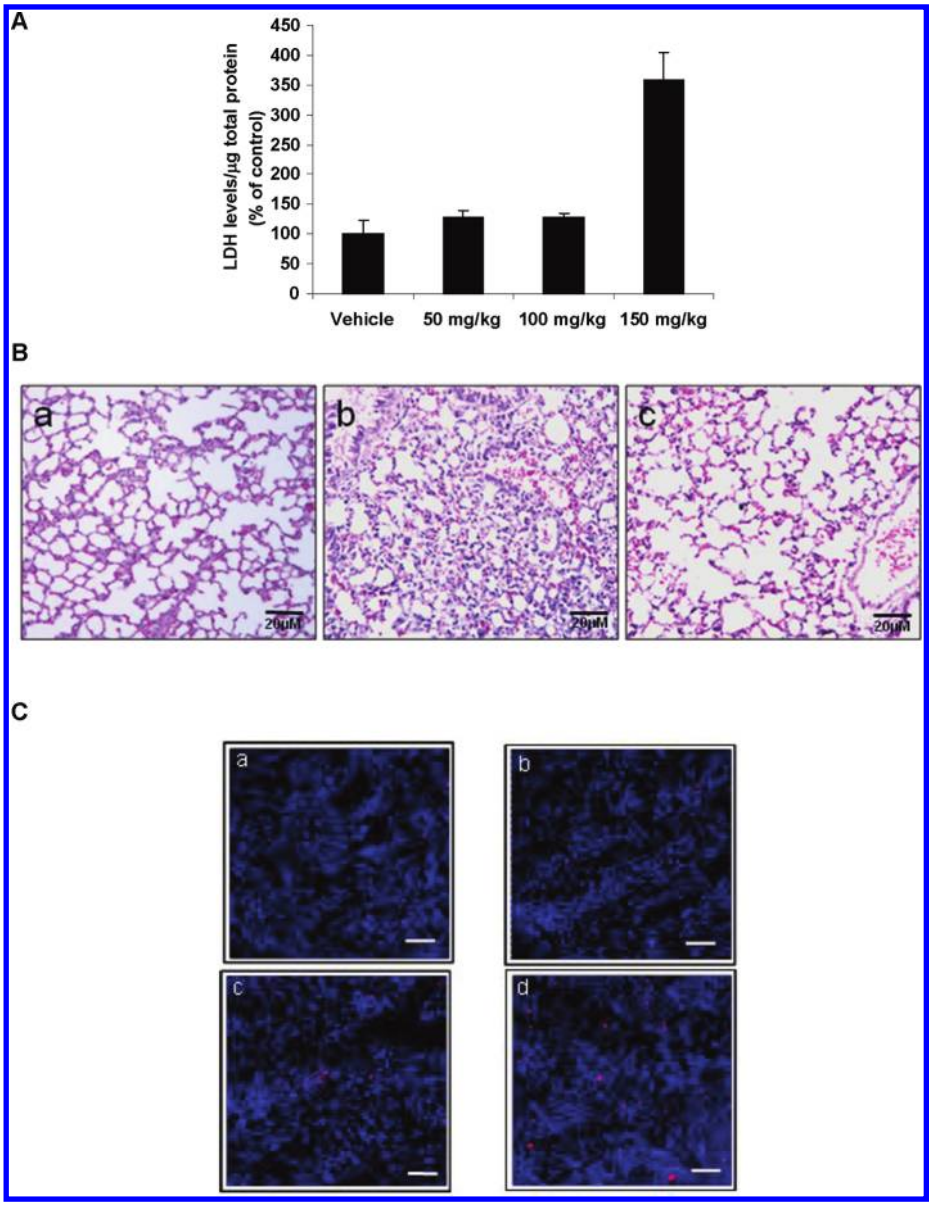

Figure 1. Toxic effects of tetrandrine on mouse lungs. (A) Changes in LDH activity in BAL fluids in CD-1 mice 24 h following ip administration of tetrandrine at doses of 0, 50, 100, and 150 mg/kg. (B) H&E stained histopathologic images of lungs from mice treated with tetrandrine (TET) at doses of 0 (a) and 150 mg/kg (b). (c) H&E stained histopathologic image of lung from mice pretreated with ketoconazole (KTC) ip at 50 mg/kg and then administered with tetrandrine ip at 150 mg/kg (200×, scale bar represents 50 μM). (C) Cell permeability: Lungs harvested from mice treated with tetrandrine at doses of 0 (a), 50 (b), 100 (c), and 150 mg/kg (d) (100×, scale bar represent 100 μm) were stained with EthD-III (in red) and nuclear fluorochrome DAPI (in blue). The former is a cell-impermeant, nuclear binding fluorochrome, and the latter is a cell-permeant nuclear binding fluorochrome with distinct spectral properties.

observed in the media where the microdissected airway tissues were exposed to tetrandrine at concentration of 100 μM for 24 h (Figure 2), relative to the vehicle-exposed group. Unlike tetrandrine, 4-ipomeanol at the same molar concentration only produced mild increase in LDH activity in the media (Figure 2).

Cell Culture and Cell Viability. Human lung WI-38 cells (a human lung fibroblast cell line) and NL-20 (a human bronchial epithelial cell line) were exposed to tetrandrine at concentrations of 5, 10, 20, and 40 μM, and cell viabilities were examined 24 h after the exposure. About 40% reduction in cell viability was observed after exposure to tetrandrine at 20 μM, and exposure to 40 μM tetrandrine caused less than 40% cell viability (Figure 3A). The same studies were performed in NL-20 cells, and similar levels of cell viability were observed (Figure 3B).

Protective Effect of Ketoconazole. Following 1.5 h ip administration of ketoconazole (50 mg/kg) or vehicle, the mice were given tetrandrine (ip, 150 mg/kg). LDH activity in BAL fluids was examined 24 h postadministration. Interestingly, the pretreatment with ketoconazole reduced LDH activity in BAL fluids induced by tetrandrine (Figure 4). Histopathologic evaluation study also revealed the similar protective effect of ketoconazole on tetrandrine-induced pulmonary toxicity. As shown in Figure 1B, the pretreatment of ketoconazole substantially reduced alveolar hemorrhage induced by tetrandrine. The observed

dx.doi.org/10.1021/tx200290s |*Chem. Res. Toxicol.* 2011, 24, 2142–2152

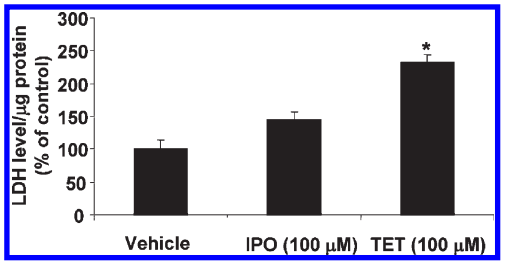

Figure 2. Toxic effects of tetrandrine on the lung airways. Changes in LDH released to media in cultured microdissected lung airways after 24 h of exposure to 4-ipomeanol (IPO, 100 μM) and tetrandrine (TET, 100 μM). Data represent three independent experiments (means ± SEMs, *<P 0.05 vs IPO).

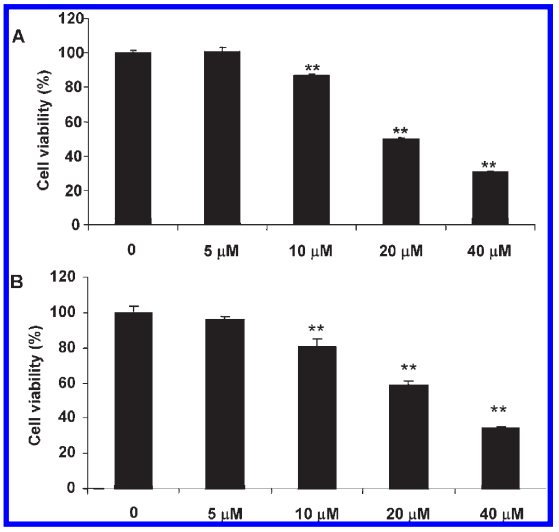

Figure 3. Cytotoxicity of tetrandrine in human lung cell lines WI-38 (A) and NL-20 (B). Cells were incubated with tetrandrine at the indicated concentrations for 24 h. Data represent the values of triplicates (means ± SEMs, *p < 0.05 vs control; **p < 0.01).

protection of ketoconazole implies that the metabolic activation may be involved in tetrandrine-induced lung injury.

Metabolic Demethylation of Tetrandrine. On the basis of the knowledge of metabolism chemistry, we speculated that *O*- or/and *N*-demethylation is/are the primary metabolism pathway(s) for tetrandrine. As an initial step for metabolic activation study, we investigated metabolic demethylation of tetrandrine. Tetrandrine was incubated with HLMs, followed by LC/MS^n analysis. A total of three demethylated metabolites with the protonated molecule $[M + H]^+$ at m/z 609 and doubly charged ion $[M + 2H]^{2+}$ at m/z 305 were detected and designated as M1, M2, and M3, respectively (Figure 5). The respective chromatographic retention times were 11.2, 12.4, and 16.9 min. To facilitate the characterization of M1-M3, the fragmentation behaviors of tetrandrine and its analogues fangchinoline (7-*O*-demethylated tetrandrine, **2**, Scheme 1) and berbamine (a diastereomer of 12-*O*-demethylated tetrandrine, **3**, Scheme 1) were evaluated by multistage mass spectrometric analysis. In the MS/MS spectrum of $[M + H]^+$ at m/z 623 (Figure 6A), tetrandrine displayed diagnostic fragment ion at m/z 381 formed by the cleavages of the C1−C17 and C1′−C17′ bonds with a loss of a *N*-methyl moiety at position 2 or 2′.

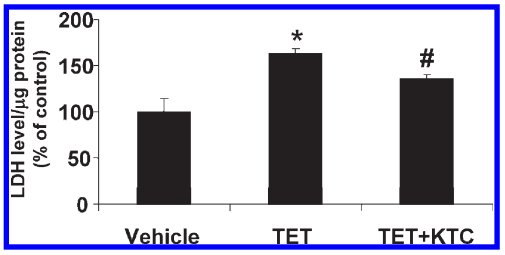

Figure 4. Protective effect of ketoconazole. Changes in LDH activity in BAL fluids. Mice were given vehicle or tetrandrine (TET). Mice pretreated intraperitoneally with ketoconazole (KTC) at 50 mg/kg for 1.5 h were administered with tetrandrine (KTC + TET). Data represent the values of six replicates (means ± SEMs, *<p 0.05 vs vehicle treated; #<p 0.05 vs TET-treated only).

Fragment ions at m/z 592 (the base peak) and 580 were formed by the elimination of CH_3NH_2 (−31 Da with a proton shift) and $CH_3N{=}CH_2$ (−43 Da with a proton shift). Fangchinoline showed similar MS fragmentation behaviors as that of tetrandrine. The observed characteristic fragment ions included m/z 578, 566, and 367 (Figure 6B), which are 14 Da lower than the three respective fragments (m/z 592, 580, and 381) of tetrandrine detected (Figure 6A). Berbamine has the same numbers of methyl group on the isoquinoline rings as that of tetrandrine. As expected, fragment ion m/z 381 was observed in its MS/MS spectrum (Figure 6C).

The observed characteristic fragments of the authentic standards of the three alkaloids, including tetrandrine, fangchinoline, and berbamine, allow us to propose the sites for the metabolic demethylation of tetrandrine to M1−M3 as follows. M1 is assigned as 12-*O*-demethylated tetrandrine (**5**, a diastereomer of berbamine, Scheme 2), since it had the same diagnostic fragment ions at m/z 381, 566, and 578 (Figure 6D) as berbamine did (Figure 6C). The fragment ion m/z 367 was observed as the base peak in MS/MS spectrum of M2 (Figure 6E). MS/MS spectrum of fangchinoline showed the fragment ion m/z 367 (Figure 6B), but its retention time (t_R = 13.0 min) differed from that of M2 (t_R = 12.4 min). Thus, *O*-demethylation at C-7 may be excluded, and M2 is likely either **6a** or **6b** (Scheme 2). In the MS/MS spectrum of M3 (Figure 6F), a neutral loss of 17 Da (NH_3) was observed, indicating the lack of methyl group on that nitrogen.[31] The diagnostic fragment ions at m/z 381 and 367 were also found, which both were derived from the cleavage of the C1−C17 or C1′−C17′ bond. Therefore, M3 is assigned as either 2-*N*-demethylated or 2′-*N*-demethylated tetrandrine (**7a** or **7b**, Scheme 2).

Quinone Methide Metabolite of Tetrandrine Trapped with GSH. The metabolic *O*-demethylation of tetrandrine detected above produced metabolites M1 and M2 (**5** and **6**, Scheme 2) with a *para*-methylene phenol and *para*-methine phenol moiety, respectively. We anticipated that these demethylated metabolites would be further biotransformed to the corresponding quinone methides. Tetrandrine was incubated with NADPH-supplemented HLMs incorporated with nucleophilic GSH to trap the quinone methide intermediates. One peak assigned as M4 at t_R = 14.5 min responsible for the corresponding GSH conjugate ($[M + 2H]^{2+}$ at m/z 458; $[M + H]^+$ at m/z 914) was detected by LC/MS^n in the incubation mixture. The formation of M4 in the incubations was NADPH-dependent, as illustrated by the representative chromatograms from human liver microsomal incubations (Figure 7).

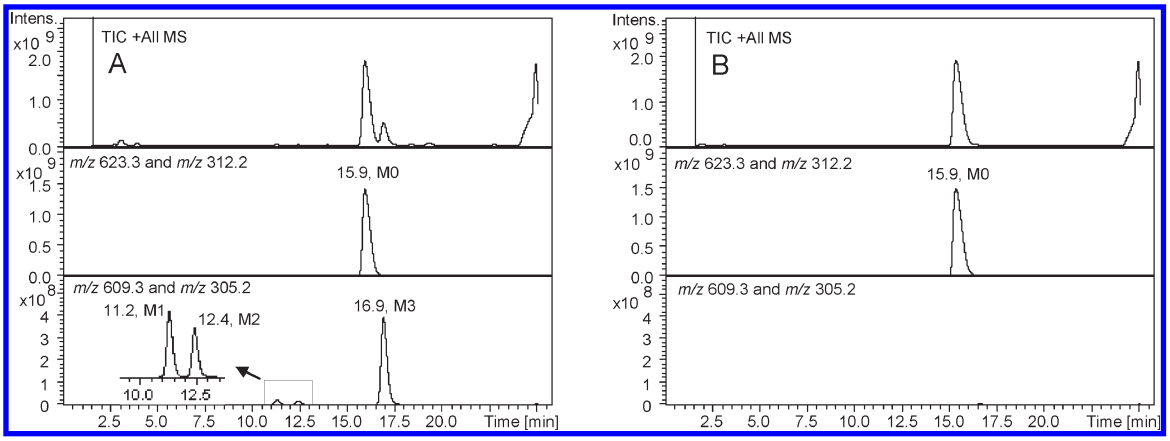

Figure 5. Extracted ion $[M + H]^+$ and $[M + 2H]^{2+}$ chromatograms of tetrandrine demethylated metabolites (labeled as M1 − M3) in human liver microsomal incubation with NADPH (A) and without NADPH (B). The parent compound is labeled as M0.

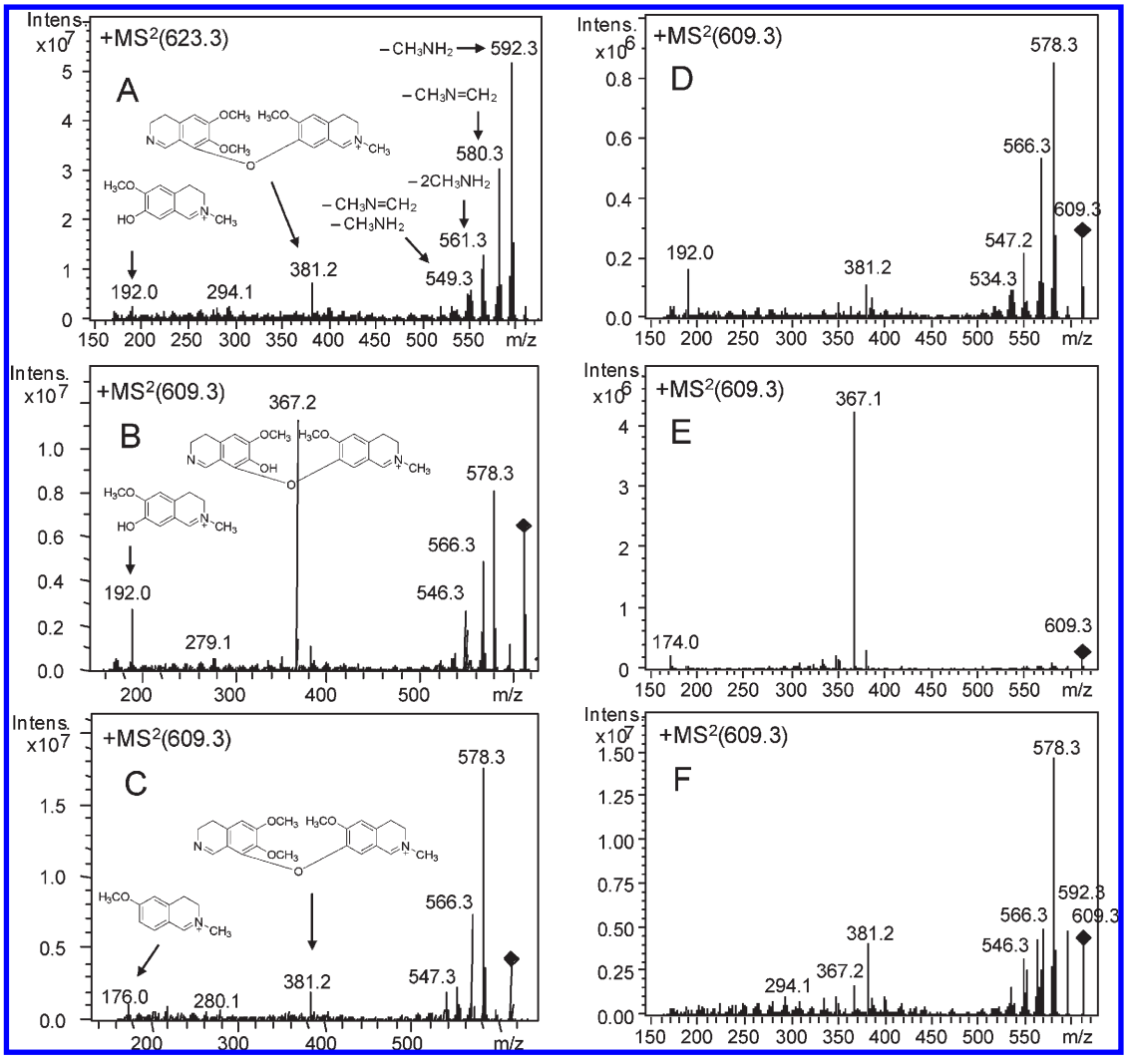

Figure 6. MS/MS spectra of tetrandrine (A), fangchinoline (B), and berbamine (C) and demethylated tetrandrine metabolites M1 (D), M2 (E), and M3 (F).

Multistage MS analysis was performed with an ion trap instrument to further characterize the GSH conjugate. M4 was detected predominantly as a doubly charged ion $[M + 2H]^{2+}$ at *m/z* 458, which is equivalent to the molecular mass of 913 Da. The observed molecular mass was 305 Da higher than that of demethylated tetrandrine, indicating an addition of one molecule

Scheme 2. Proposed Metabolic Formation of GSH Conjugate from Tetrandrine in Human Liver or Mouse Lung Microsomal Incubations Supplemented with NADPH and GSH

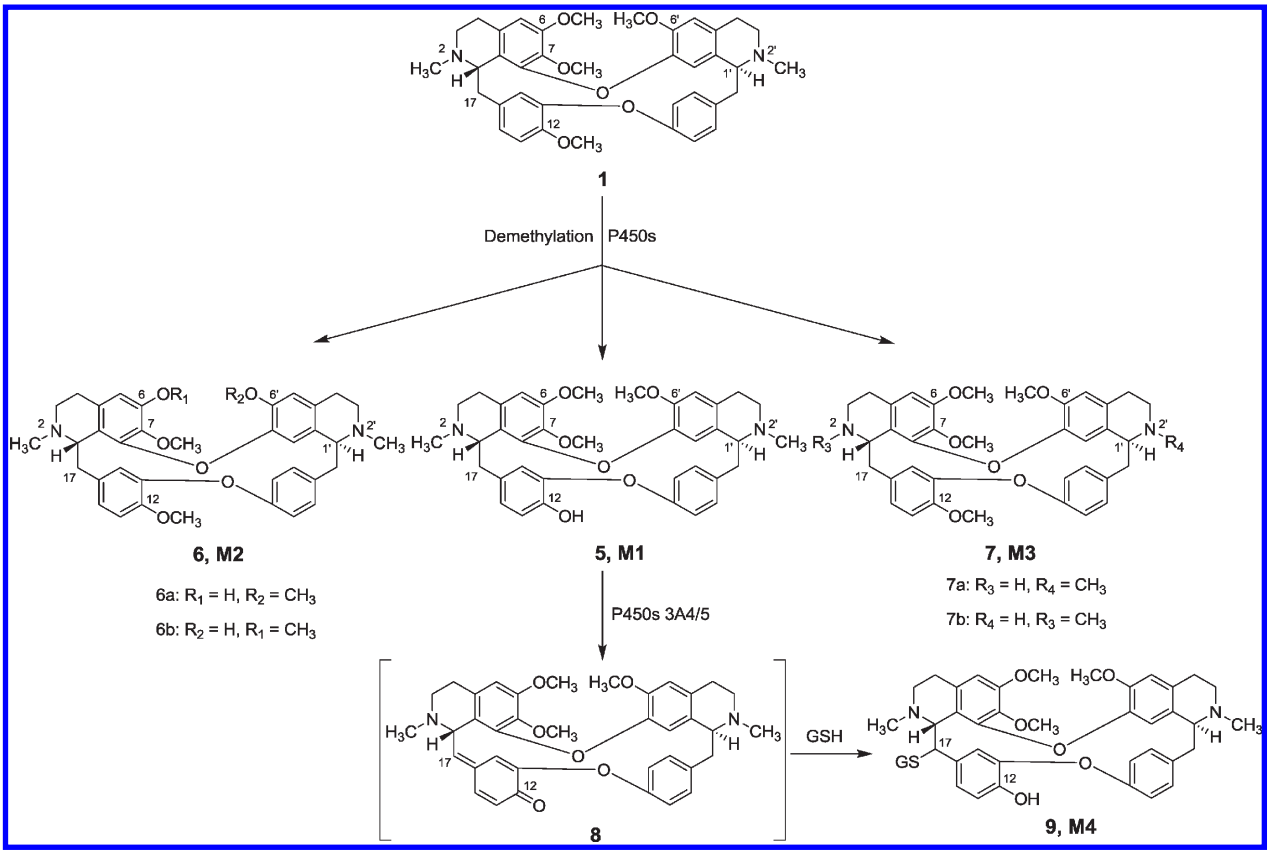

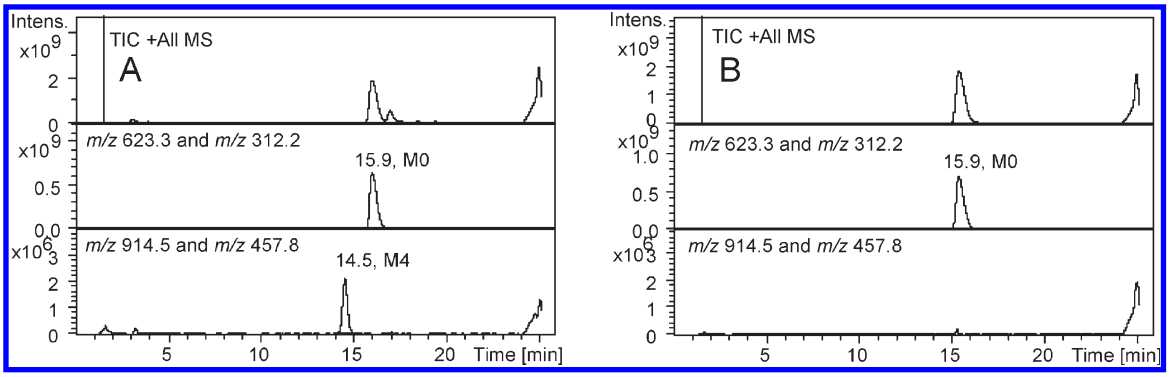

Figure 7. Extracted ion $[M + H]^+$ and $[M + 2H]^{2+}$ chromatograms of *O*-demethylated tetrandrine GSH conjugate (labeled as M4) in human liver microsomal incubations with NADPH and GSH (A) and with GSH but without NADPH (B).

of GSH to the demethylated tetrandrine. The MS/MS spectrum of M4 showed product ions at *m/z* 785 (−129 Da, −pyroglutamate), 641 (−273 Da, −(GSH−H_2S)), 607 (−307 Da, −GSH), and 381. The MS^3 spectrum (*m/z* 458 ($[M+2H]^{2+}$) → 607) displayed fragment ion *m/z* 381, where the neutral losses were coincident with those observed in MS/MS spectrum of 12-*O*-demethylated tetrandrine (Figure 8).

Identification of P450 Enzymes Responsible for Bioactivation of Tetrandrine. Tetrandrine was incubated with HLMs as above. The participation of P450 enzymes in bioactivation of tetrandrine was probed by coincubation with individual P450 enzyme-selective inhibitors, including ketoconazole (P450 3A), α-naphthoflavone (P450 1A2), sulfaphenazole (P450 2C9), ticlopidine (P450 2B6/0.4 μM and P450 2C19/6.0 μM), quinidine (P450 2D6), or chlormethiazole (P450 2E1). The formation of M4 was monitored in the microsomal reactions in the presence or the absence of the individual inhibitors. The presence of ketoconazole (1.0 μM) significantly reduced the formation of M4 in the microsomal mixtures (Figure S1 in the Supporting Information). No such inhibition was observed in the microsomal incubations in the presence of the other inhibitors.

dx.doi.org/10.1021/tx200290s |*Chem. Res. Toxicol.* 2011, 24, 2142–2152

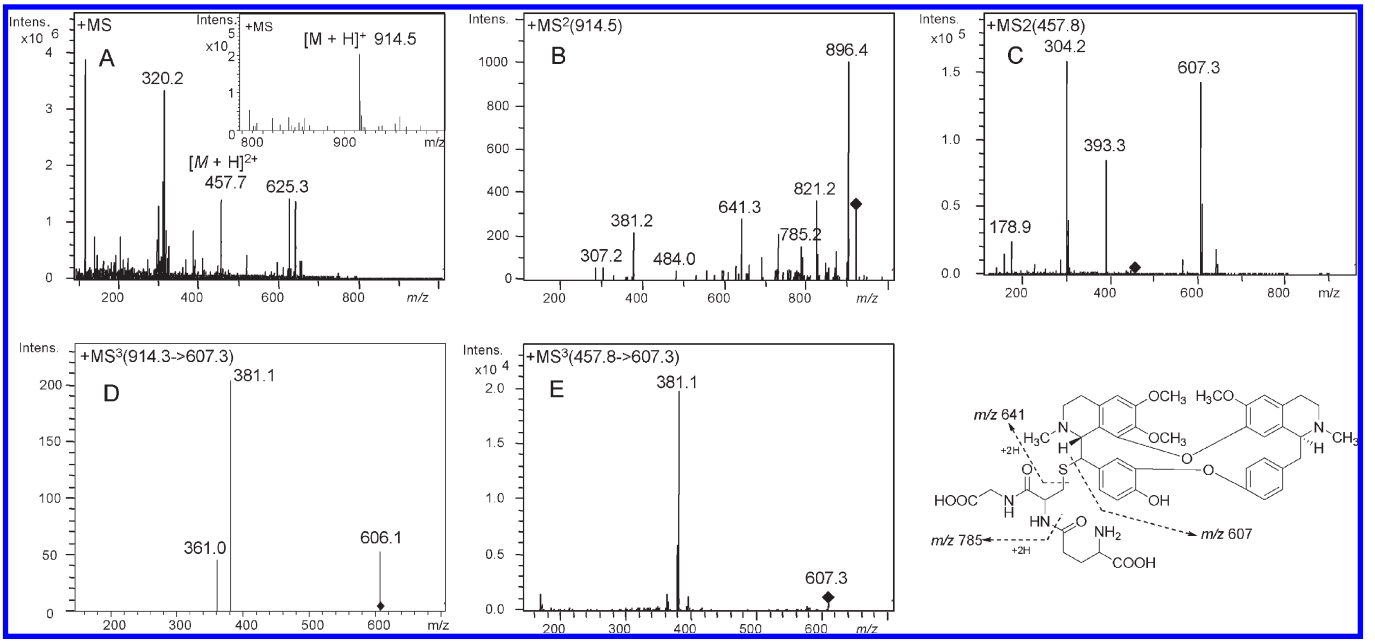

Figure 8. Mass spectrometry analysis of *O*-demethylated tetrandrine GSH conjugate (M4) in HLMs. (A) Full scan mass spectrum, (B) MS/MS spectrum of $[M + H]^+$ at m/z 914, (C) MS/MS spectrum of $[M + 2H]^{2+}$ at m/z 458, (D) MS^3 spectrum of m/z 914 → 607, and (E) MS^3 spectrum of m/z 458 ($[M + 2H]^{2+}$) → 607.

In a separate study, tetrandrine was incubated with individual recombinant human P450s 1A2, 1B1, 2A6, 2B6, 2C8, 2C9, 2C19, 2D6, 2E1, 3A4, 3A5, and 4A11, mixed with GSH as the trapping agent. As expected, GSH conjugate M4 was detected in the incubations only with P450s 3A4 or 3A5. There was no such product detected in the incubations with the other P450 enzymes, as depicted in Figure S2 in the Supporting Information. The results were consistent with the observation obtained in the microsomal enzyme inhibition studies above.

Bioactivation of Tetrandrine in Mouse Lung Microsomes. The observed protective effect of ketoconazole on tetrandrine-induced lung injury in mice encouraged us to investigate metabolic activation of tetrandrine in mouse lungs, although bioactivation of tetrandrine was evident in HLMs (Figures 7 and 8). Tetrandrine was incubated with CD-1 mouse lung microsomes in the presence or absence of NADPH, and the resulting electrophilic metabolites were trapped with GSH, followed by LC/MS^n analysis. As expected, a single peak responsible M4 (m/z 914; retention time, 14.5 min) was observed in samples from the incubations in the presence of NADPH (Figure 9), while no such peak was detected in the samples from the NADPH-absent incubations. The effect of ketoconazole on the bioactivation of tetrandrine was examined, and the presence of ketoconazole (1.0 μM) in mouse lung microsomal incubations caused substantial reduction (40% based on peak areas) in the formation of M4 as shown in Figure 9.

Enzymatic Oxidation of *O*-Demethylated Tetrandrine. *O*-Demethylated tetrandrine was hypothesized to be the precursor of M4. To probe our hypothesis, we isolated M1 from up-scaled human liver microsomal reactions with tetrandrine and sequentially incubated the purified metabolite with mouse lung microsomes trapped with GSH. As expected, M4 was detected in the microsomal reactions (Figure S3 in the Supporting Information). The absence of NADPH in the microsomal incubations failed to produce the GSH conjugate. Additionally, coincubation of ketoconazole

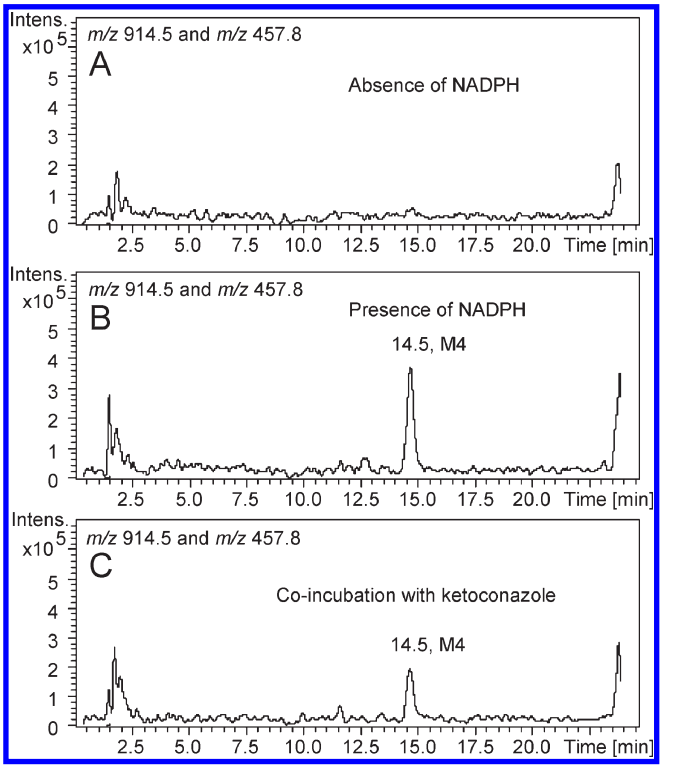

Figure 9. Extracted ion $[M + H]^+$ and $[M + 2H]^{2+}$ chromatograms of M4 in mouse lung microsomal incubation with tetrandrine trapped with GSH without NADPH (A), with NADPH (B), and with NADPH and ketoconazole (1.0 μM; C).

(1.0 μM) in mouse lung microsomal incubations caused substantial suppression (35% based on peak areas) of M4 formation. A similar study was performed with M2, but no GSH conjugate

dx.doi.org/10.1021/tx200290s |*Chem. Res. Toxicol.* 2011, 24, 2142–2152

M4 was detected in the mouse lung microsomal reactions (Figure S3D in the Supporting Information).

DISCUSSION

Multiple administration of tetrandrine at 40 mg/kg for 2 months reportedly induced hepatotoxicity in dogs.[28] Tetrandrine is used in China as an antirheumatism agent, and the suggested dose is 60−120 mg/day with warning of possible liver injury. A recent report indicated tetrandrine at 150 mg/kg was given in rats for antitumor treatment.[32] A careful toxicity evaluation is needed for the safety of possibly expanded use of tetrandrine. Our present study showed that single doses of tetrandrine at 150 mg/kg ip did not change serum ALT and AST activities in mice 24 h following administration (Figure S4 in the Supporting Information), suggesting that the alkaloid did not cause acute liver damage in this model. Instead, increased numbers of ethidium-positive (Figure 1C) cells were observed in the lungs obtained from the mice treated with the same dose of tetrandrine, while lungs of the control animals showed no detectable ethidium-labeled cells. The ethidium labeling of lung cells exhibited dose dependency for tetrandrine (Figure 1C). Histopathologic evaluation of lungs of mice showed that tetrandrine at 150 mg/kg caused significant alveolar edema and hemorrhage (Figure 1B). These results provide clear evidence that tetrandrine induces acute lung injury.

Ketoconazole showed protection against pulmonary toxicity of tetrandrine in mice (Figures 1B and 4), implicating that metabolic activation is involved in tetrandrine-induced pulmonary toxicity. This led us to investigate the metabolic activation of tetrandrine in the pulmonary system. Tetrandrine was incubated with mouse lung microsomes, and a demethylated tetrandrine−derived reactive metabolite trapped with GSH to M4 was detected in the microsomal reactions (Figure 9). Additionally, we evaluated the pulmonary toxicity of tetrandrine in cultured microdissected mouse airways. The LDH activity in the incubation media was monitored as a biomarker of tissue injury. A 2-fold increase in LDH released from the tissues was observed after exposure to tetrandrine at 100 μM (Figure 2). The observed toxicity of tetrandrine in our in vitro model indicates that tetrandrine can execute its pulmonary toxicity within pulmonary system, not relying on other organs. The pulmonary toxicity of 4-ipomeanol, a prototype selective pulmonary toxicant, was assessed in the same tissue culture model. In this model system of exposure, 4-ipomeanol induced only mild elevation of LDH activity in the media at the same molar concentration (Figure 2). The studies in vivo and in vitro clearly demonstrated that tetrandrine is a potent toxin to pulmonary system.

Quinone methides were speculated to be potential reactive metabolites of tetrandrine, based on our earlier dauricine work.[30,31] Dauricine (**4a**, Scheme 1) is a monoether type bisbenzylisoquinoline alkaloid with similar structure as that of tetrandrine. Dauricine was found to be bioactivated to the corresponding quinone methide (**4b**, Scheme 1), and ip administration of dauricine produced lung injury.[30,31] Structurally, tetrandrine does not have *para*-methylene phenol moiety, the precursor of quinone methide, but such a functional group can be virtually generated through metabolic *O*-demethylation. A total of three demethylated tetrandrine metabolites were detected in human liver microsomal reactions with tetrandrine (Figure 5). M1 is assigned as 12-*O*-demethylated tetrandrine (**5**, Scheme 2), based on the observed similarity between the MS/MS spectra of M1 and that of berbamine (Figure 6C,D), a diastereomer of 12-*O*-demethylated tetrandrine. Particularly, the MS/MS spectra of M1 and berbamine shared the same characteristic fragment ion at m/z 381.

An electrophilic metabolite trapped by GSH designated as M4 was detected by LC/MS^n, following both human liver and mouse lung microsomal incubations with tetrandrine in the presence of NADPH and GSH (human lung microsomal studies were not pursued, due to a lack of appropriate sample sources). In LC/MS^n analysis, the MS/MS spectrum of M4 showed the neutral losses of 129 Da (pyroglutamate), 273 Da (GSH-H_2S), and 307 Da (GSH). This provides the evidence for the formation of a GSH conjugate. In the MS^3 spectrum of M4, characteristic fragment ion at m/z 381 was observed (Figure 8C), and fragment m/z 381 was also shown in the MS^2 spectrum of M1 (Figure 6D). This implies that the alkaloid part is derived from 12-*O*-demethylated tetrandrine. In addition, M4 was detected in NADPH- and GSH-supplemented mouse lung microsomal incubations with purified M1. This provides additional evidence that M1 is the precursor of M4. We anticipate that the resulting *para*-methylene phenol of M1 was sequentially metabolized to the corresponding quinone methide (**8**, Scheme 2), which further reacted with GSH applied in the microsomal incubations. The quinone methide intermediate may react with GSH via 1,2-, 1,4-, or 1,6-addition to form the GSH conjugate detected by LC-MS (labeled as M4, Figures 7 and 9). Unfortunately, the limited quantity of the resultant GSH conjugate made it difficult to gain an NMR spectrum for the determination of the site where GSH conjugation takes place. We propose that the nucleophilic reaction of GSH occurs on the exocyclic methylene to form 17-glutathionyl-12-*O*-demethylated tetrandrine (**9**, Scheme 2), based on our previous dauricine work[30,31] and other literatures.[33−35]

The formation of GSH conjugate M4 was found to require NADPH, and the absence of NADPH in human liver and mouse lung microsomal incubations failed to produce M4 after exposure to tetrandrine. In addition, the coincubation of ketoconazole suppressed the formation of M4 (Figures 9C and S1 in the Supporting Information). These results provided clear evidence for the metabolic activation of tetrandrine. The effect of ketoconazole on tetrandrine-induced pulmonary toxicity was also evaluated, and the animal study demonstrated that pretreatment with ketoconazole attenuated the pulmonary toxicity of the alkaloid (Figures 1B and 4). The observed protective effect of ketoconazole on pulmonary toxicity of tetrandrine, combined with the suppressive effect of ketoconazole on the formation of quinone methide **8** in microsomal reactions with tetrandrine, suggests the participation of metabolic activation of tetrandrine in the pulmonary toxicity induced by the alkaloid. Catalytic activities of a total of 12 recombinant human cytochrome P450 enzymes in bioactivation of tetrandrine were evaluated, and only P450s 3A4 and 3A5 were found to biotransform tetrandrine to quinone methide **8**, trapped by GSH to conjugate M4 (Figure S1 in the Supporting Information). However, it was uncertain that the conversion of 12-*O*-demethylated tetrandrine (**5**) to quinone methide **8** occurred spontaneously or enzymatically. To differentiate the two processes, we incubated purified M1 with GSH-supplemented mouse lung microsomes in the presence or absence of NADPH as well as ketoconazole. The formation of the GSH conjugate required NADPH and was inhibited by ketoconazole. The results indicate that P450 3A subfamily catalyzes the *O*-demethylation of tetrandrine to M1 and the sequential dehydrogenation

of M1 to quinone methide **8** (Scheme 2). P450 3A4 is mainly expressed in human liver but little in the lung,[36] while P450 3A5 is the major enzyme of P450 3A subfamily expressed in human pulmonary system.[36] It is most likely that P450 3A5 is the enzyme responsible for the metabolic activation of tetrandrine in pulmonary system if P450 3A family participates in the bioactivation of tetrandrine in humans. Quinone methide **8** was also detected in mouse lung microsomal incubations with tetrandrine, and coincubation of ketoconazole suppressed the formation of the quinone methide (Figure 9). This indicates the participation of P450 3A family in catalysis of the bioactivation of tetrandrine in mouse lung.[37]

Quinone methides are known electrophilic species reactive to nucleophilic molecules. Toxicities of quinone methides as reactive metabolites have been documented, including acute cytotoxicity, immunotoxicity, and carcinogenesis.[38−40] As highly redox active molecules, quinones can participate in redox cycle with their semiquinone radicals, leading to the formation of reactive oxygen species. Additionally, quinones as Michael receptors can alkylate cellular nucleophilic macromolecules such as proteins and DNA. Studies have also demonstrated that some quinones and hydroquinones can poison topoisomerase II.[41,42] The mechanisms of the observed selective pulmonary toxicity of tetrandrine remain unknown. One explanation for the liver resistance to acute tetrandrine toxicity may include the higher capacity of hepatic GSH against the attack by the quinone methide metabolite.

In conclusion, single intraperitoneal doses of tetrandrine at 150 mg (0.24 mmmol)/kg induced pulmonary toxicity in CD-1 mice. Pretreatment with P450 3A subfamily selective inhibitor ketoconazole reduced the susceptibility of animals to pulmonary toxicity of tetrandrine. Microsomal reactions of tetrandrine generated an electrophilic metabolite, most likely a quinone methide metabolite. Ketoconazole suppressed the bioactivation of tetrandrine to the reactive metabolite. The observed protective effect of ketoconazole on pulmonary toxicity by tetrandrine, along with the observation of the suppressive effect of ketoconazole on the formation of the reactive metabolite of tetrandrine, implicates the involvement of metabolic activation of tetrandrine in the pulmonary toxicity induced by tetrandrine.

■ ASSOCIATED CONTENT

Supporting Information. Figures of effects of P450 inhibitors and isoforms on the formation of GSH conjugate M4, extracted ion chromatograms of M4 in mouse lung microsomal incubations, and changes in serum ALT and AST in mice given tetrandrine. This material is available free of charge via the Internet at http://pubs.acs.org.

■ AUTHOR INFORMATION

Corresponding Author

*Tel/Fax: +86-21-50800738. E-mail: xychen@mail.shcnc.ac.cn (X.C.). Tel: 206-884-7651. Fax: 206-987-7660. E-mail: jiang.zheng@seattlechildrens.org (J. Z.).

Author Contributions

§These authors equally contributed to the work.

Funding Sources

This work was partially supported by Grant #30873119 of the National Natural Science Foundation of China.

■ ACKNOWLEDGMENT

We thank Andrew Lowe for his assistance in the preparation of this manuscript.

■ ABBREVIATIONS

ALT, alanine aminotransferase; AST, aspartate aminotransferase; BAL, bronchoalveolar lavage; BHT, butylated hydroxytoluene; DAPI, 4′,6-diamidino-2-phenylindole; DMEM, Dulbecco's modified Eagle's medium; EIC, extracted ion chromatogram; ESI, electrospray ionization; EthD-III, ethidium homodimer-III; GSH, glutathione; H&E, hematoxylin and eosin; HLMs, human liver microsomes; LC/MS^n, liquid chromatography/ion trap mass spectrometry; LDH, lactate dehydrogenase; P450, cytochrome P450; PBS, phosphate-buffered saline.

■ REFERENCES

(1) Yang, X. Y., Jiang, S. Q., Zhang, L., Liu, Q. N., and Gong, P. L. (2007) Inhibitory effect of dauricine on inflammatory process following focal cerebral ischemia/reperfusion in rats. *Am. J. Chin. Med. 35*, 477–486.

(2) Lin, H., Wang, Y., Xiong, Z., Tang, Y., and Liu, W. (2007) Effect of antenatal tetrandrine administration on endothelin-1 and epidermal growth factor levels in the lungs of rats with experimental diaphragmatic hernia. *J. Pediatr. Surg. 42*, 1644–1651.

(3) Li, Y. H., and Gong, P. L. (2007) Neuroprotective effects of dauricine against apoptosis induced by transient focal cerebral ischaemia in rats via a mitochondrial pathway. *Clin. Exp. Pharmacol. Physiol. 34*, 177–184.

(4) Li, Y. H., and Gong, P. L. (2007) Neuroprotective effect of dauricine in cortical neuron culture exposed to hypoxia and hypoglycemia: involvement of correcting perturbed calcium homeostasis. *Can. J. Physiol. Pharmacol. 85*, 621–627.

(5) Zhao, X., Cui, X. Y., Chen, B. Q., Chu, Q. P., Yao, H. Y., Ku, B. S., and Zhang, Y. H. (2004) Tetrandrine, a bisbenzylisoquinoline alkaloid from Chinese herb Radix, augmented the hypnotic effect of pentobarbital through serotonergic system. *Eur. J. Pharmacol. 506*, 101–105.

(6) Lohombo-Ekomba, M. L., Okusa, P. N., Penge, O., Kabongo, C., Choudhary, M. I., and Kasende, O. E. (2004) Antibacterial, antifungal, antiplasmodial, and cytotoxic activities of *Albertisia Villosa*. *J. Ethnopharmacol. 93*, 331–335.

(7) He, Q. Y., Meng, F. H., and Zhang, H. Q. (1996) Reduction of doxorubicin resistance by tetrandrine and dauricine in harringtonineresistant human leukemia (HL60) cells. *Acta Pharmacol. Sin. 17*, 179–181.

(8) Marshall, S. J., Russell, P. F., Wright, C. W., Anderson, M. M., Phillipson, J. D., Kirby, G. C., Warhurst, D. C., and Schiff, P. L., Jr. (1994) In vitro antiplasmodial, antiamoebic, and cytotoxic activities of a series of bisbenzylisoquinoline alkaloids. *Antimicrob. Agents Chemother. 38*, 96–103.

(9) Angerhofer, C. K., Guinaudeau, H., Wongpanich, V., Pezzuto, J. M., and Cordell, G. A. (1999) Antiplasmodial and cytotoxic activity of natural bisbenzylisoquinoline alkaloids. *J. Nat. Prod. 62*, 59–66.

(10) Kwan, C. Y., and Achike, F. L. (2002) Tetrandrine and related bisbenzylisoquinoline alkaloids from medicinal herbs: Cardiovascular effects and mechanisms of action. *Acta Pharmacol. Sin. 23* (12), 1057–1068.

(11) Choi, H. S., Kim, H. S., Min, K. R., Kim, Y., Lim, H. K., Chang, Y. K., and Chung, M. W. (2000) Anti-inflammatory effects of fangchinoline and tetrandrine. *J. Ethnopharmacol. 69*, 173–179.

(12) Lai, J. H. (2002) Immunomodulatory effects and mechanisms of plant alkaloid tetrandrine in autoimmune diseases. *Acta Pharmacol. Sin. 23*, 1093–1101.

(13) Ho, L. J., Juan, T. Y., Chao, P., Wu, W. L., Chang, D. M., Chang, S. Y., and Lai, J. H. (2004) Plant alkaloid tetrandrine downregulates IjBa kinases-IjBa-NF-jB signaling pathway in human peripheral blood T cell. *Br. J. Pharmacol. 143*, 919–927.

(14) Rao, M. R. (2002) Effects of tetrandrine on cardiac and vascular remodeling. *Acta Pharmacol. Sin. 23*, 1075–1085.
(15) Park, P. H., Nan, J. X., Park, E. J., Kang, H. C., Kim, J. Y., Ko, G., and Sohn, D. H. (2000) Effect of tetrandrine on experimental hepatic fibrosis induced by bile duct ligation and scission in rats. *Pharmacol. Toxicol. 87*, 261–268.
(16) Elsharkawy, A. M., Oakley, F., and Mann, D. A. (2005) The role and regulation of hepatic stellate cell apoptosis in reversal of liver fibrosis. *Apoptosis 10*, 927–939.
(17) Hsu, Y. C., Chiu, Y. T., Cheng, C. C., Wu, C. F., Lin, Y. L., and Huang, Y. T. (2007) Antifibrotic effects of tetrandrine on hepatic stellate cells and rats with liver fibrosis. *J. Gastroenterol. Hepatol. 22*, 99–111.
(18) Zhou, H. Y., Wang, F., Cheng, L., Fu, L. Y., Zhou, J., and Yao, W. X. (2003) Effects of tetrandrine on calcium and potassium currents in isolated rat hepatocytes. *World J. Gastroenterol. 9*, 134–136.
(19) Dong, Y., Yang, M. M., and Kwan, C. Y. (1997) *In vitro* inhibition of proliferation of HL-60 cells by tetrandrine and corlolus versicolor peptide derived from chinese medicinal herbs. *Life Sci. 60*, 135–140.
(20) Wang, G., Lemos, J. R., and Iadecola, C. (2004) Herbal alkaloid tetrandrine: from an ion channel blocker to inhibitor of tumor proliferation. *Trends Pharmacol. Sci. 25*, 120–123.
(21) Chen, Y., Chen, J. C., and Tseng, S. H. (2009) Tetrandrine suppresses tumor growth and angiogenesis of gliomas in rats. *Int. J. Cancer 124*, 2260–2269.
(22) Chen, Y. J. (2002) Potential role of tetrandrine in cancer therapy. *Acta Pharmacol. Sin. 23*, 1102–1106.
(23) Choi, S. U., Park, S. H., Kim, K. H., and Choi, E. J. (1998) The bis benzylisoquinoline alkaloids, tetrandine and fangchinoline, enhance the cytotoxicity of multidrug resistance-related drugs via modulation of P-glycoprotein. *Anti-Cancer Drugs 9*, 255–261.
(24) Fu, L. W., Zhang, Y. M., Liang, Y. J., Yang, X. P., and Pan, Q. C. (2002) The multidrug resistance of tumour cells was reversed by tetrandrine *in vitro* and in xenografts derived from human breast adenocarcinoma MCF-7/adr cells. *Eur. J. Cancer 38*, 418–426.
(25) Liu, Z. L., Hirano, T., Tanaka, S., Onda, K., and Oka, K. (2003) Persistent reversal of P-glycoprotein-mediated daunorubicin resistance by tetrandrine in multidrug-resistant human T lymphoblastoid leukemia MOLT-4 cells. *J. Pharm. Pharmacol. 55*, 1531–1537.
(26) Fu, L. W. Y. J., Deng, L. W., Ding, Y., Chen, L. M., Yanli Ye, Y. L., Yang, X. P., and Pan, Q. C. (2004) Characterization of tetrandrine, a potent inhibitor of P-glycoprotein-mediated multidrug resistance. *Cancer Chemother. Pharmacol. 53*, 349–356.
(27) Chen, B. A., Sun, Q., Wang, X. M., Gao, F., Dai, Y. Y., Yin, Y., Ding, J. H., Gao, C., Cheng, J., Li, J. Y., Sun, X. C., Chen, N. N., Xu, W. L., Shen, H. L., and Liu, D. L. (2008) Reversal in multidrug resistance by magnetic nanoparticle of Fe_3O_4 loaded with adriamycin and tetradrine in K562/A02 leukemic cells. *Int. J. Nanomed. 3*, 277–286.
(28) Li, T. L., Hu, T. Y., Zou, C. Q., Yao, P. P., and Zheng, Q. (1982) Studies of the chronic toxicity of tetrandrine in dogs: An inhibitor of silicosis. *Ecotoxicol. Environ. Saf. 6*, 528–534.
(29) Cai, Y., Qi, X. M., Gong, L. K., Liu, L. L., Chen, F. P., Xiao, Y., Wu, X. F., Li, X. H., and Ren, J. (2006) Tetrandrine-induced apoptosis in rat primary hepttocytes is initiated from mitochondria: Caspases and Endonuclease G (Endo G) pathway. *Toxicology 218*, 1–12.
(30) Jin, H., Dai, J. Y., Chen, X. Y., Liu, J., Zhong, D. F., Gu, Y. S., and Zheng, J. (2010) Pulmonary toxicity and metabolic activation of dauricine in CD-1 mice. *J. Pharmacol. Exp. Ther. 332*, 738–746.
(31) Wang, Y. Y., Zhong, D. F., Chen, X. Y., and Zheng, J. (2009) Identification of quinone methide metabolites of dauricine in human liver microsomes and in rat bile. *Chem. Res. Toxicol. 22*, 824–834.
(32) Chen, Y., Chen, J. C., and Tseng, S. H. (2009) Tetrandrine suppresses tumor growth and angiogenesis of gliomas in rats. *Int. J. Cancer 15*, 2260–2269.
(33) Thompson, D. C., Perera, K., Krol, E. S., and Bolton, J. L. (1995) O-Methoxy-4-alkylphenols that form quinone methides of intermediate reactivity are the most toxic in rat liver slices. *Chem. Res. Toxicol. 8*, 323–327.
(34) Monks, T. J., and Jones, D. C. (2002) The metabolism and toxicity of quinones, quinonimines, quinone methides and quinone-thioethers. *Curr. Drug. Metab. 3*, 425–438.
(35) Lindsey, R. H. J., Bender, R. P., and Osheroff, N. (2005) Effect of benzene metabolites on DNA cleavage mediated by human topoisomerase IIR: 1, 4-hydroquinone is a topoisomerase II poison. *Chem. Res. Toxicol. 18*, 761–770.
(36) Anttila, S., Hukkanen, J., Hakkola, J., Stjernvall, T., Beaune, P., Edwards, R. J., Boobis, A. R., Pelkonen, O., and Raunio, H. (1997) Expression and localization of CYP3A4 and CYP3A5 in human lung. *Am. J. Respir. Cell Mol. Biol. 16*, 242–249.
(37) Pelkonen, O., Turpeinen, M., Hakkola, J., Honkakoski, P., Hukkanen, J., and Raunio, H. (2008) Inhibition and induction of human cytochrome P450 enzymes: Current status. *Arch. Toxicol. 82*, 667–715.
(38) Bolton, J. L., Trush, M. A., Penning, T. M., Dryhurst, G., and Monks, T. J. (2000) Role of quinones in toxicology. *Chem. Res. Toxicol. 13*, 135–160.
(39) Monks, T. J., and Jones, D. C. (2002) The metabolism and toxicity of quinones, quinonimines, quinone methides and quinone-thioethers. *Curr. Drug Metab. 3*, 425–438.
(40) Baillie, T. A. (2008) Metabolism and toxicity of drugs. Two decades of progress in industrial drug metabolism. *Chem. Res. Toxicol. 21*, 129–137.
(41) Bender, R. P., Lindsey, R. H. J., Burden, D. A., and Osheroff, N. (2004) *N*-Aceyl-*P*-benzoquinone imine, the toxic metabolite of acetaminophen, is a topoisomerase II poison. *Biochemistry 43*, 3731–3739.
(42) Lindsey, R. H. J., Bender, R. P., and Osheroff, N. (2005) Effect of benzene metabolites on DNA cleavage mediated by human topoisomerase II α 1, 4-hydroquinone is a topoisomerase II poison. *Chem. Res. Toxicol. 18*, 761–770.